

# Quasiparticle thermal Hall angle and magnetoconductance in $\text{YBa}_2\text{Cu}_3\text{O}_x$ .

K. Krishana, N. P. Ong, Y. Zhang, and Z. A. Xu<sup>†</sup>

*Joseph Henry Laboratories of Physics, Princeton University, Princeton, New Jersey 08544*

R. Gagnon and L. Taillefer<sup>§</sup>

*Department of Physics, McGill University, Montreal, Quebec, Canada*

(May 19, 2019)

We present a way to extract the quasiparticle (*qp*) thermal conductivity  $\kappa_e$  and mean-free-path in  $\text{YBa}_2\text{Cu}_3\text{O}_x$ , using the thermal Hall effect and the magnetoconductance of  $\kappa_e$ . The results are very consistent with heat capacity experiments. Moreover, we find a simple relation between the thermal Hall angle  $\theta_Q$  and the  $H$ -dependence of  $\kappa_e$ , as well as numerical *equality* between  $\theta_Q$  and the electrical Hall angle. The findings also reveal an anomalously anisotropic scattering process in the normal state.

74.25.Fy, 74.72.Bk, 72.15.Gd, 74.60.Ge

The quasiparticle excitations in cuprate superconductors display many unusual properties related to their long transport lifetimes and the existence of nodes in the gap function. These properties have been investigated by microwave and heat transport techniques. Bonn *et al.* [1] uncovered a broad peak in the zero-field microwave conductivity in  $\text{YBa}_2\text{Cu}_3\text{O}_7$  (YBCO). From measurements of the zero-field thermal conductivity anomaly in untwinned YBCO, Yu *et al.* [2] inferred that it arises entirely from the quasiparticles. Taillefer *et al.* [3] measured values of  $\kappa_{xx}$  below 0.1 K that are close to the predicted universal value  $\kappa_e^{00}$  [4].

The long quasiparticle lifetime also produces a large thermal Hall effect which has been investigated in YBCO [5]. While the quasiparticles are solely responsible for the thermal Hall conductivity  $\kappa_{xy}$ , their contribution to the diagonal conductivity  $\kappa_{xx}$  is harder to sort out experimentally. The general problem of *qp* transport in a  $d$ -wave superconductor in a field is an active area of research [4,6–9]. Novel effects such as those arising from the doppler-shift term [7], field quantization of the states around the nodes [8], and Andreev scattering from a disordered vortex array [9] have been proposed.

We report results that reveal a close relation between  $\kappa_{xy}$  and  $\kappa_{xx}$  in YBCO. We find that the thermal Hall angle  $\theta_Q$  closely tracks a parameter  $p(T)$  extracted from the field dependence of  $\kappa_{xx}$ , which implies strongly that  $p(T)$  is proportional to the *qp* mean-free-path (*mfp*). In addition, we find that  $\theta_Q$  agrees *numerically* with the electrical Hall angle  $\theta_e$  extrapolated from above  $T_c$ . Our results disagree with the factor of 2 discrepancy found in a recent related study [10].

Measurements of  $\kappa_{xx}$  and  $\kappa_{xy}$  were made on 4 crystals (1-4) in a field  $\mathbf{H} \parallel \mathbf{c}$ . Samples 1 and 2 are both optimally doped and detwinned with  $x = 6.95$  and  $T_c = 93.3$  K. With the thermal current  $\mathbf{J}_Q \parallel \hat{\mathbf{x}} \parallel \mathbf{a}$ , the thermal gradient  $-\partial_x T$  is measured with a pair of matched cernox sensors. The antisymmetric ‘Hall’ gradient  $-\partial_y T \parallel \mathbf{b}$  (the chain axis) is measured with a pair of chromel-constantan thermocouples, as in [5]. Samples 3 and 4 are underdoped

twinned crystals with  $T_c = 63$  and 60 K, respectively (in both  $x = 6.63$ ).

As our analysis rests on the finding that  $\kappa_{ph}$  (the phonon conductivity) is insensitive to  $H$ , we first summarize the evidence for this result. In the cuprates, the field dependence of  $\kappa_{xx}$  is known to be described by the equation

$$\kappa_{xx}(H, T) = \frac{\kappa_e^0(T)}{(1 + p(T)|H|)} + \kappa_B(T), \quad (1)$$

where  $p(T)$  is an inverse field scale.

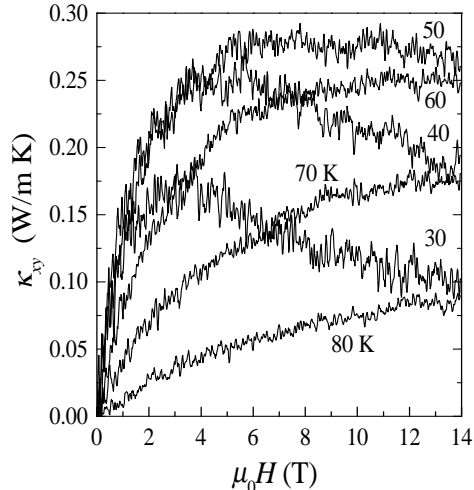


FIG. 1. The Hall conductivity  $\kappa_{xy}$  in untwinned  $\text{YBa}_2\text{Cu}_3\text{O}_7$  (sample 1), with thermal current  $\mathbf{J}_Q \parallel \mathbf{a}$  and  $\mathbf{H} \parallel \mathbf{c}$ .

Equation 1 has been tested at high resolution. In underdoped YBCO (in which  $p(T)$  approaches  $4 \text{ T}^{-1}$  at 10 K), it was found that  $\kappa_{xx}$  fits Eq. 1 to a precision of 1 part in  $10^3$  over 2 decades in  $H$  *provided*  $\kappa_B$  is  $H$ -independent [11]. This is especially clear below 20 K, where  $\kappa_{xx}$  attains an  $H$ -independent (to the stated resolution) plateau value in underdoped YBCO [11]. The key

point is that the best fits are obtained with a background term  $\kappa_B$  that is  $H$ -independent. Thus, these earlier findings impose the constraint that either the  $qp$  conductivity or the phonon conductivity must be  $H$ -independent.

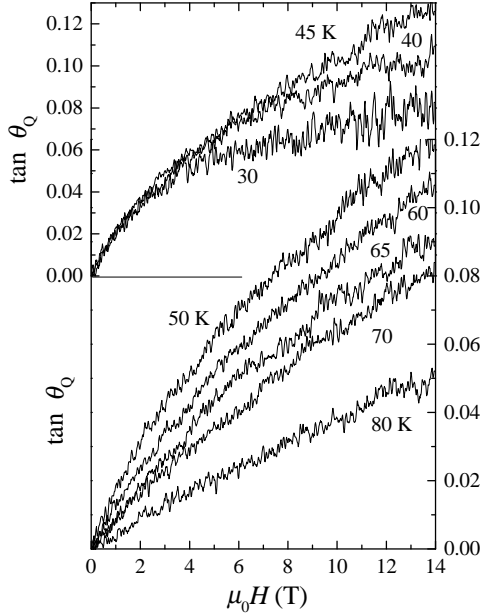


FIG. 2. Traces of the Hall angle  $\tan \theta_Q = \kappa_{xy}/\kappa_e$  where  $\kappa_e \equiv \kappa_{xy} - \kappa_B$ , with  $\kappa_B$  determined by fitting to Eq. 1 (sample 1).

Because  $\kappa_{xy}$  displays strong curvature vs.  $H$ , the phonon term is clearly the one that is  $H$ -independent. Hence, in Eq. 1, we identify the difference  $\kappa_{xx} - \kappa_B$  with the field-dependent part of the  $a$ -axis  $qp$  conductivity  $\kappa_{e,a}(H, T)$  (we have written  $\kappa_e^0 = \kappa_{e,a}(0, T)$ ). The  $H$ -independent term  $\kappa_B$  is identified with  $\kappa_{ph}$ , including possibly a very small residual electronic term  $\kappa_e^{00}$  that is  $H$ -independent [9]. With  $\kappa_{e,a}$  so extracted, we may obtain the thermal Hall angle  $\tan \theta_Q \equiv \kappa_{xy}(H, T)/\kappa_{e,a}(H, T)$  (hereafter we drop the  $a$  in  $\kappa_{e,a}$ ).

The Hall conductivity  $\kappa_{xy}$  in sample 1 (see Fig. 1) displays behavior similar to that in Ref. [5], but with stronger curvature vs.  $H$ . Results for samples 2 are closely similar. Combining  $\kappa_{xy}$  and the parameters in Eq. 1, we derive  $\tan \theta_Q$ . The traces in Fig. 2 show that  $\tan \theta_Q$  is initially linear in  $H$ , but displays increasing curvature at large  $H$  and low  $T$ . We focus only on the initial value.

The weak-field  $\tan \theta_Q$  provides a powerful clue to the meaning of  $p(T)$ . Comparing the two quantities (main panel of Fig. 3), we note that  $p(T)$  increases rapidly with decreasing  $T$ , closely tracking  $\theta_Q$ . Between 30 and 80 K, the data for  $p(T)$  and  $\theta_Q$  (open triangles) may be made to lie on the same curve, if we simply divide  $p(T)$  by the dimensionless scale factor  $\mathcal{M} \equiv p(T)B/\theta_Q$  ( $B \rightarrow 0$ ) (in both 1 and 2,  $\mathcal{M}$  equals 13). Thus, the two quantities share the same  $T$  dependence over a broad range of  $T$ .

As  $\tan \theta_Q$  is generally proportional to the  $qp$  lifetime,

the comparison implies that  $p(T)$  is also proportional to the  $qp$  lifetime or mean-free-path  $\ell(T)$ . It is then convenient to express  $p(T)$  in the general form

$$p(T) = \ell(T)s/\phi_0, \quad (2)$$

where the length scale  $s$  depends on the particular model, and  $\phi_0 = h/2e$  ( $h$  is Planck's constant and  $e$  is the elementary charge).

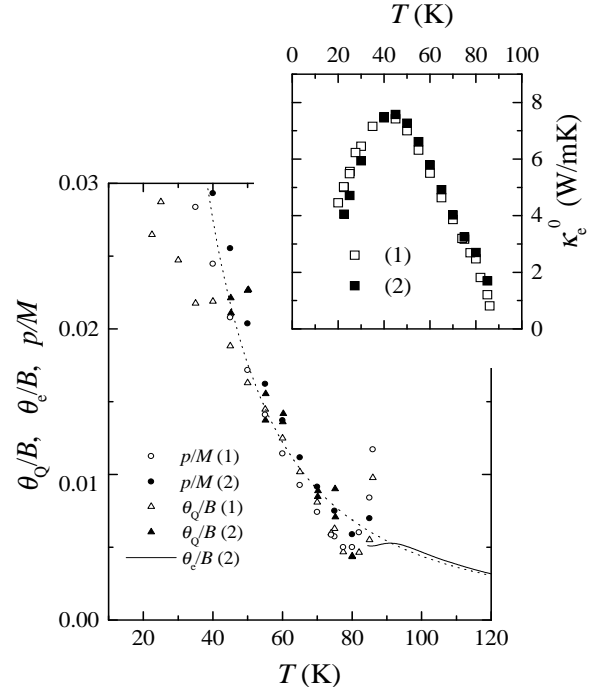


FIG. 3. [Main panel] Comparison of the parameter  $p(T)/\mathcal{M}$  in samples 1 (open circles) and 2 (solid circles), with the weak-field  $\theta_Q/B$  in 1 (open triangles) and 2 (solid triangles). The solid line are values of  $\theta_e/B$  measured in sample 2 above 93 K (the broken line shows its extrapolation as the curve  $44/T^2$ ). The inset shows the zero-field  $qp$  conductivity  $\kappa_e^0$  extracted in 1 and 2.

We may also express the initial Hall-angle in terms of a 'Hall-angle' mean-free-path  $\ell_H$ , viz.  $\theta_Q = \ell_H(T)eB/\hbar k_F$  with  $k_F$  the Fermi wavevector. Proportionality between  $p(T)$  and  $\tan \theta_Q$  implies

$$s = (\ell_H/\ell)(\mathcal{M}\pi/k_F) \simeq 65(\ell_H/\ell) \text{ Å}, \quad (3)$$

with  $k_F \simeq 0.64 \text{ Å}^{-1}$ .

We add the caveat that, in 93-K YBCO, the simple proportionality between  $p(T)$  and  $\ell$  expressed in Eq. 2 does not hold close to  $T_c$ . Above 80 K, the extracted  $p(T)$  and  $\theta_Q$  appear to diverge as  $T \rightarrow T_c^-$ . This divergence is an artifact produced by the existence of a sharp zero-field cusp in the  $\kappa_{xx} - H$  profile close to  $T_c$  (its presence enhances the slope of  $\kappa_{xx}$  vs.  $H$  as  $H \rightarrow 0$ ). In 93-K YBCO, the cusp smoothly merges into the regular profile and cannot be isolated easily. Thus, the apparent  $p(T)$  is increasingly distorted as we get close to  $T_c$ . However,

in underdoped YBCO, the cusp is clearly distinct from the regular profile and its effect may be subtracted (see inset in Fig. 4). The origin of the cusp is unknown at present.

Recent heat capacity experiments on YBCO place strong constraints on the analysis of  $\kappa_e^0$  at low  $T$ , which we now address. The  $qp$  thermal conductivity  $\kappa_e^0$  ( $H=0$ ) extracted for samples 1 and 2 are displayed in the inset in Fig. 3. As  $T$  decreases,  $\kappa_e^0$  increases by  $\sim 10$  before decreasing rapidly. We may write  $\kappa_e^0 = c_e \langle v\ell \rangle / 2$  where  $c_e$  is the electronic heat capacity and  $\langle v\ell \rangle$  denotes the group velocity- $mfp$  product averaged over the Fermi Surface. The weak-field Hall conductivity is  $(c_e \langle v\ell \rangle / 2) \tan \theta_Q$ . At low  $T$  in a  $d$ -wave superconductor, the Boltzmann-equation approach gives  $\langle v\ell \rangle = (v_1 \ell_1 + v_2 \ell_2) / 2$ , where subscripts 1 and 2 refer to the principal axes of the Dirac cone at the nodes (as  $v_1/v_2 \simeq 7$ , transport along the 1-axis dominates). Dividing the two conductivities by  $\ell_1$  and  $\ell_1^2$ , respectively, gives quantities that may be compared with  $c_e$ . Although  $p(T)$  in our experiment determines  $\ell_1$  only up to the unknown parameter  $s$ , we may plot our data as  $\kappa_e^0/p(T)$  and  $\kappa_{xy}(0)/Bp(T)^2$ , and examine their  $T$  dependence (Fig. 4). Below 60 K, both are consistent with a power-law  $T$  dependence (in particular,  $\kappa_{xy}(0)/Bp(T)^2$  fits a  $T^2$  behavior).

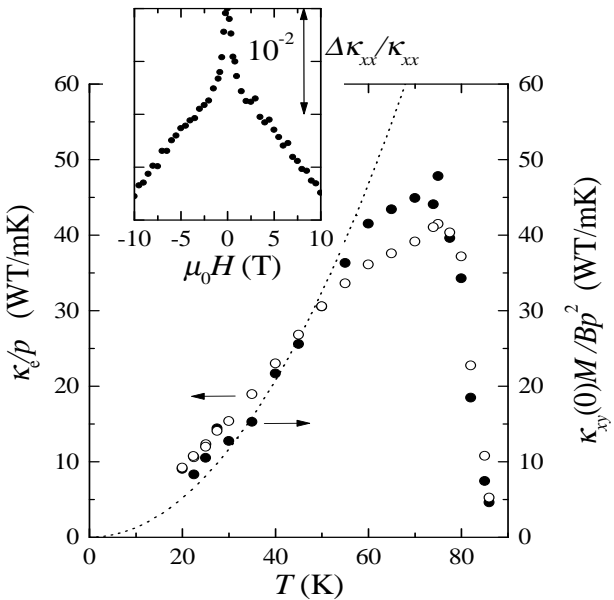


FIG. 4. (Main panel) The  $T$  dependence of  $\kappa_e/p(T)$  (open circles) and  $\kappa_{xy}(0)/Bp(T)^2$  (solid circles) in sample 1. Both quantities are proportional to  $c_e$  ( $\kappa_{xy}(0)$  is multiplied by  $\mathcal{M}$ ). From the value of  $\alpha$  reported by Wright *et al.*, we have calculated  $\kappa_e^0/\ell_1$ , and plotted it as  $(\kappa_e^0/\ell_1) \times (\phi_0/s)$  with  $s = 45 \text{ \AA}$  (the broken line =  $0.013 T^2 \text{ TW/Km}$ ). The inset shows the cusp anomaly in  $\kappa_{xx}$  vs.  $H$  at 55 K in underdoped YBCO.

The heat capacity measurements appear to be converging to the result that, at  $H=0$ ,  $c_e$  varies as  $\alpha T^2$  at low  $T$ , with  $\alpha \simeq 0.064 \text{ mJ K}^{-3} \text{ mol}^{-1}$  [13]. This value of  $\alpha$  implies [14]  $v_1 = v_F = 1.78 \times 10^7 \text{ cm/s}$  and  $\kappa_e^0/\ell_1 = 2.72 \times 10^4 \text{ T}^2$ .

By comparing the second equation with our results, we can fix the unknown scale  $s$ . The best fit (broken line in Fig. 4) gives  $s = 45 \text{ \AA}$ , in good agreement with Eq. 3. With this  $s$  in Fig. 3, we find that  $\ell_1 \simeq 1,800 \text{ \AA}$  at 40 K.

We next compare the  $T$  dependence of  $\tan \theta_Q$  with the electrical Hall angle  $\tan \theta_e = \rho_{xy}/\rho_b$  (the solid line in Fig. 3, main panel). Remarkably,  $\tan \theta_Q$  falls on the  $1/T^2$  curve of  $\tan \theta_e$  extrapolated to below 93 K with no adjustments to either scale (dotted line). In YBCO, a large fraction ( $\sim 1/2$ ) of the charge carriers are in the chains ( $\parallel \mathbf{b}$ ). Because of the resistivity anisotropy  $\rho_a/\rho_b$  ( $=2.1$  at 100 K), it is important that we compare  $\tan \theta_Q$  with the correct Hall angle  $\rho_{xy}/\rho_b$  (this probes the electrical current  $\parallel \mathbf{a}$ ; the incorrect choice  $\rho_{xy}/\rho_a$  is only half as large). Hence, our finding of numerical agreement between  $\tan \theta_Q$  and  $\tan \theta_e$  applies strictly to the carriers in the  $\text{CuO}_2$  plane. The case for  $\mathbf{J}_Q \parallel \mathbf{b}$  remains to be investigated. Nevertheless, when twinned crystals are used (see 3 and 4), we still observe *equality* between the two Hall angles. This suggests that the equality holds as well when  $\mathbf{J}_Q \parallel \mathbf{b}$ . Thus, our overall finding is inconsistent with that of Zeini *et al.* who find that  $\theta_Q/\theta_e \simeq 2$  in a twinned crystal [10].

The results in the underdoped 60-K crystals provide important complementary information. We may extend measurements of  $p(T)$  to lower  $T$  (10 K) because flux pinning is much weaker. Further, the cusp near  $T_c$  is readily separated from the regular  $H$  dependence of  $\kappa_{xx}$  (inset of Fig. 4), so  $p(T)$  may be reliably determined up to  $T_c$ . In the main panel of Fig. 5, we display  $p(T)$  measured in samples 3 and 4 (open triangles and circles, respectively). With increasing  $T$ ,  $p(T)$  falls rapidly. The  $T$  dependence of  $\theta_Q$  (solid symbols) is closely similar. By adjusting  $\mathcal{M}$  ( $= 20$  and  $15$  for samples 3 and 4, respectively), we may also match the curves for  $\theta_Q$  and  $p(T)$ . We emphasize that  $p(T)$  does not show a divergence near  $T_c$ , unlike the case in 1 and 2. Moreover, as  $T$  increases above 55 K,  $p(T)/\mathcal{M}$  falls *below* the curve for  $\theta_e/B$ . Also shown are data for the electrical Hall angle  $\theta_e$  measured in 4 (crosses).

In the inset in Fig. 5, we display the same data over a broader range of  $T$  (10 to 240 K). The log-log plot shows that  $\theta_Q$  continues on the curve for  $\theta_e$  extrapolated below  $T_c$  (without any scale adjustment). Between  $T_c$  and 100 K, the upper curve displays an apparent broad minimum. This shallow feature is the superposition of a rapidly decreasing  $\tan \theta_e$  (as  $T \rightarrow T_c^+$ ) and a rapidly increasing  $\tan \theta_Q$  as  $T$  decreases below  $T_c$ . A recent investigation reveals that the decrease in  $\tan \theta_e$  is correlated with the opening of the pseudogap at 150 K [15]. This causes the Hall angle to plummet steeply relative to its high- $T$  trend. The inset shows rather clearly that, apart from the dip,  $\theta_Q$  is continuous with the normal-state  $\theta_e$ .

It is instructive to re-express the underdoped results in terms of mean-free-paths. Over the interval 30-55 K,  $\ell$  and  $\ell_H$  are proportional. If we assume  $\ell \simeq \ell_H$ , we may use the scale factor  $\mathcal{M}$  to convert  $p(T)$  and  $\theta_Q$  into  $mfp$ 's. In the inset in Fig. 5 (right axis) we have expressed  $p(T)$

and  $\theta_Q$  in terms of  $\ell$ . We find that  $\ell$  decreases rapidly from 4,000 to 550 Å between 10 and 50 K. Above  $T_c$ , however,  $\ell$  and  $\ell_H$  follow different curves.

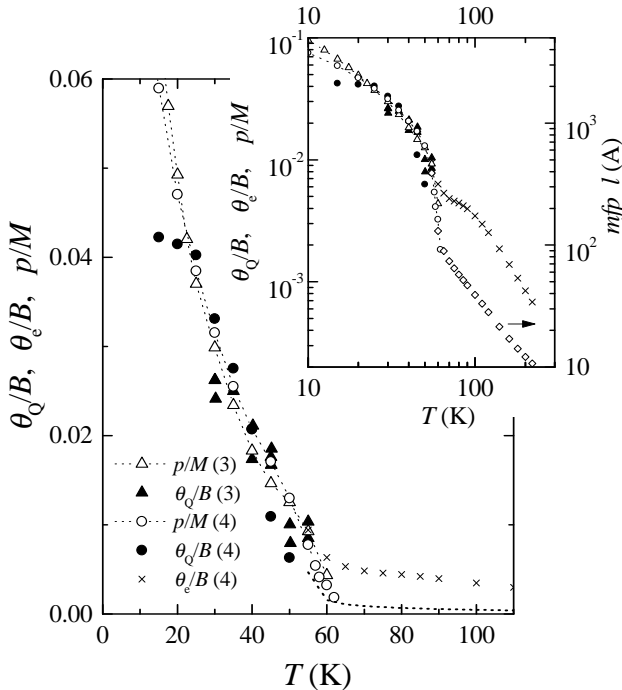


FIG. 5. [Main panel] The  $T$  dependence of  $p(T)/\mathcal{M}$  (open symbols) and  $\theta_Q/B$  (solid symbols) in underdoped YBCO (samples 3 and 4). Data for  $\theta_e/B$  above 60 K (from 4) are shown as an  $\times$ . The inset shows the same data in log-log scale to emphasize that  $\theta_Q$  is continuous with  $\theta_e$  except for a ‘dip’ between 60 and 100 K associated with the opening of the pseudogap. The right axis represents the data in terms of  $\ell$  and  $\ell_H$  (see text). The diamonds are values for  $\ell$  obtained from the in-plane  $\rho$  measured in 4 (also shown as a dotted line in main panel).

Whereas  $\ell_H$  smoothly joins the  $1/T^2$  Hall-angle curve in the normal state,  $\ell$  derived from  $p(T)$  sharply decreases across  $T_c$  (open symbols), assuming values above 55 K much shorter than  $\ell_H$ . The sharp reduction in  $\ell$  is consistent with the transport  $mfp$  (diamonds) deduced from the in-plane resistivity  $\rho$  [16]. It appears that, starting about 10 K below  $T_c$ , a novel scattering mechanism  $\Gamma_{tr}$  becomes prominent and grows rapidly with  $T$ . It selectively damps the longitudinal current, but does not seem to affect the transverse (Hall) current. Thus,  $\ell$  decreases more rapidly than  $\ell_H$  across  $T_c$ , resulting in the two branches shown in the inset of Fig. 5. The two branches are the  $mfp$  versions of the two lifetimes previously extracted from the Hall angle and resistivity by Chien *et al.*, following a proposal by Anderson [17]. It remains to be seen if conventional models employing hot spots can reproduce the observed split.

In summary, we have combined measurements of  $\kappa_{xx}$  vs.  $H$  with  $\kappa_{xy}$  to achieve a self-consistent separation of the  $qp$  and phonon conductivities. The numerical agree-

ment between the thermal and electrical Hall angles in both twinned and untwinned crystals, and the comparison with heat capacity experiments support the validity of the analysis presented.

We thank P. W. Anderson, M. Franz, and F.D.M. Haldane for many discussions. N.P.O. acknowledges support from the U.S. Office of Naval Research (N00014-90-J-1013) and the U.S. National Science Foundation (DMR98-09483).

<sup>†</sup> Permanent address of ZAX: Department of Physics, Zhejiang University, Hangzhou, China.

<sup>§</sup> Present address of LT: Department of Physics, University of Toronto, Toronto, Ontario, Canada M5S 1A7.

---

- [1] D. A. Bonn *et al.*, Phys. Rev. Lett. **68**, 2390 (1992); D. A. Bonn *et al.*, Phys. Rev. B **50**, 4051 (1994); W. N. Hardy *et al.*, Phys. Rev. Lett. **70**, 3999 (1993).
- [2] R. C. Yu, M. B. Salamon, Jian Ping Lu, and W. C. Lee, Phys. Rev. Lett. **69**, 1431 (1992).
- [3] L. Taillefer *et al.*, Phys. Rev. Lett. **79**, 483 (1997).
- [4] P. A. Lee, Phys. Rev. Lett. **71**, 1887 (1993).
- [5] K. Krishana, J. M. Harris, and N. P. Ong, Phys. Rev. Lett. **75**, 3529 (1995).
- [6] Steve H. Simon and Patrick A. Lee, Phys. Rev. Lett. **78**, 1548 (1997).
- [7] C. Kubert and P. J. Hirschfeld, Phys. Rev. Lett. **80**, 4693 (1998).
- [8] Philip W. Anderson, cond-mat/9812063.
- [9] M. Franz, Phys. Rev. Lett. *in press*, cond-mat/9808230.
- [10] B. Zeini *et al.*, Phys. Rev. Lett. *in press*. The factor of 2 discrepancy in Zeini’s work may arise from their starting assumption that  $\tan \theta_Q$  is strictly  $H$ -linear (see our Fig. 2).
- [11] K. Krishana, Y. Zhang, Z. A. Xu, and N. P. Ong, *to be published*.
- [12] Xiao-Gang Wen and Patrick A. Lee, Phys. Rev. Lett. **80**, 2193 (1998); P. A. Lee and X. G. Wen, *ibid.* **78**, 4111 (1997).
- [13] D. A. Wright *et al.*, Phys. Rev. Lett. **82**, 1550 (1999). The spread of values found for  $\alpha$  is discussed by Wright *et al.*
- [14] At low  $T$ ,  $c_e$  is given by  $4\eta k_B^3 T^2 / (\pi d \hbar^2 v_F v_2)$ , where  $d = 5.8$  Å,  $v_F$  and  $v_2$  are the principal-axis velocities, and  $\eta = \int_0^\infty dx x^3 (-\partial f / \partial x) \simeq 5.41$ . With  $v_F/v_2 = 7$ , we find  $v_F = 1.78 \times 10^7$  cm/s.
- [15] Z.A. Xu, Y. Zhang, and N. P. Ong, cond-mat/990312.
- [16] From the measured  $\rho$  (70  $\mu\Omega\text{cm}$  at 70 K), we find  $k_F \ell = 22$ , which gives a lower bound to the  $mfp$  of 34 Å. We estimate that near the nodes  $\ell$  is about 3 times larger.
- [17] P. W. Anderson, Phys. Rev. Lett. **67**, 2092 (1991); T. R. Chien *et al.*, Phys. Rev. Lett. **67**, 2088 (1991).